

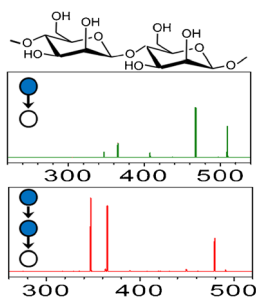
Simple Approach for De Novo Structural Identification of Mannose Trisaccharides

Hsu Chen Hsu,¹ Chia Yen Liew,¹ Shih-Pei Huang,^{1,2} Shang-Ting Tsai,¹ Chi-Kung Ni^{1,3}

¹Institute of Atomic and Molecular Sciences, Academia Sinica, P. O. Box 23-166, Taipei, 10617, Taiwan

²Department of Chemistry, National Taiwan Normal University, Taipei, 11677, Taiwan

³Department of Chemistry, National Tsing Hua University, Hsinchu, 30013, Taiwan



Abstract. Oligosaccharides have diverse functions in biological systems. However, the structural determination of oligosaccharides remains difficult and has created a bottleneck in carbohydrate research. In this study, a new approach for the de novo structural determination of underivatized oligosaccharides is demonstrated. A low-energy collision-induced dissociation (CID) of sodium ion adducts was used to facilitate the cleavage of desired chemical bonds during the dissociation. The selection of fragments for the subsequent CID was guided using a procedure that we built from the understanding of the saccharide dissociation mechanism. The linkages, anomeric configurations, and branch locations of oligosaccharides were determined by comparing the CID spectra of oligosaccharide with the fragmentation patterns based on the dissociation mechanism and our specially prepared disaccharide CID spectrum database. The usefulness of this method was demonstrated to determine the structures of several mannose trisaccharides. This method can also be applied in the structural determination of oligosaccharides larger than trisaccharides and containing hexose other than mannose if authentic standards are available.

Keywords: Oligosaccharide, Structure, CID

Received: 28 September 2017/Revised: 6 November 2017/Accepted: 9 November 2017/Published Online: 12 December 2017

Introduction

Carbohydrates (or glycans) are one of the four major classes of biomolecules. They are commonly found on cellular surfaces and extracellular matrixes and are influential in all cellular recognition processes and many other biological processes [1, 2]. To determine the relationship between the chemical and biological properties of carbohydrates, the structures of carbohydrates must be identified. However, this remains a challenge [3] because of the heterogeneity of carbohydrates and only small quantities can be extracted from biological systems. Most importantly, the number of carbohydrate isomers for a given chemical formula is significantly high, which makes the structural identification of carbohydrates through a single analytical method very difficult. For example, the number of all possible oligosaccharide isomers containing six hexoses was estimated [4] to be higher than 1.05×10^{12} . This high

number, known as the isomer barrier [4], is a long-standing technological problem in the structural analysis of carbohydrates.

The structures of carbohydrates can be determined through nuclear magnetic resonance spectroscopy [5] and mass spectrometry (MS) [6]. MS is widely applied in the structural analysis of carbohydrates because it requires only a small sample (typically from 100 μm to 10 nm) compared with other methods. However, the application of MS in the structural determination of carbohydrates has not been as successful as that in the structural determination of proteins, mainly because of the low ionization efficiency of carbohydrates in a mass spectrometer [7, 8], the large number of carbohydrate isomers [4], and the similarity of mass spectra between isomers.

The complete structural characterization of oligosaccharides requires the identification of the constituent monosaccharides, sequence, linkages, anomeric configurations, and branch location. Collision-induced dissociation (CID) tandem MS is a major method that employs mass spectrometry to determine the structure of carbohydrates [9]. Several empirical fragmentation patterns of carbohydrate cations [10–12], anions [13–18], and derivatized carbohydrates [19–24] have been reported

Electronic supplementary material The online version of this article (<https://doi.org/10.1007/s13361-017-1850-5>) contains supplementary material, which is available to authorized users.

Correspondence to: Chi-Kung Ni; e-mail: ckni@po.iam.s.sinica.edu.tw

and used in structural determination. However, they can only determine part of the structure or a small set of well-characterized oligosaccharides in databases.

Few methods for the de novo structural identification of carbohydrates have been reported in the literature. Nagy and Pohl demonstrated a fixed-ligand kinetic method for the absolute configuration determination of hexose monosaccharides [25], but no application of this method for the structural determination of oligosaccharides has been reported. Bendiak et al. assigned the stereochemistry and anomeric configuration of monosaccharides in oligosaccharides by using anion m/z 221 [26–28]. However, the structure of two monosaccharides on the reducing side cannot be determined, and it is only suitable for identifying linear oligosaccharides.

N- and O-linked glycans are important compounds for biological systems, as many research findings have proven that these glycans are involved in immune responses, cell-to-cell communications, cell apoptosis, and congenital disorders. N-linked glycans share a common core structure containing mannose oligosaccharides. Recently, we demonstrated a new approach for the de novo structural determination of oligosaccharides [29]. Through this method, the linkage, anomeric configuration, and branched locations of underivatized linear and branched oligosaccharides can be determined. The structural determination of mannose trisaccharides was demonstrated in this study. The approach is simple and the sensitivity level is high. Because the dissociation mechanism we used in the structural determination does not depend on the size of oligosaccharides and the orientations of hydroxyl groups, this method has the potential to be developed into a standard procedure for determining larger oligosaccharides and those containing hexoses other than mannose.

Experimental

High-Performance Liquid Chromatography-Electrospray Ionization-MSⁿ

All disaccharide CID spectra for the database were measured in the positive mode by using a linear ion trap mass spectrometer (LTQ XL, Thermo Fisher Scientific, Waltham, MA, USA) coupled with a Dionex Ultimate 3000 high-performance liquid chromatography (HPLC) system (Thermo Fisher Scientific). The Dionex chromatography mass spectrometry link was installed as an interface to control the Dionex chromatography system with Xcalibur (MS) (Thermo Fisher Scientific). Samples were prepared in ultrapure water at a concentration of 1×10^{-4} M. The ^{18}O -labeled carbohydrates were prepared using a previously described method [30].

HPLC separations of all disaccharides were performed using a Hypercarb (100×2.1 mm) column with a particle size of 3 μm , operated at room temperature (25 °C). The mobile phase comprised (A) 0.1% (v/v%) aqueous formic acid with 1×10^{-4} M NaCl, and (B) HPLC-grade acetonitrile. Various mobile phase elution conditions were carried out to optimize a superior separation for different isomers. The mobile phase

for isocratic elution was a mixture of A-B (97:3, v/v) for β -Man-(1 \rightarrow 2)-Man and β -Man-(1 \rightarrow 6)-Man, and a mixture of A-B (99:1, v/v) for α -Man-(1 \rightarrow 3)-Man, α -Man-(1 \rightarrow 4)-Man, α -Man-(1 \rightarrow 6)-Man, and β -Man-(1 \rightarrow 4)-Man. The solvent gradient employed for α -Man-(1 \rightarrow 2)-Man, and β -Man-(1 \rightarrow 3)-Man separation consisted of a linear increase in the amount of acetonitrile (B) in solvent A. The gradient mode conditions for α -Man-(1 \rightarrow 2)-Man were as follows: $t = 0$ min, A: 100%, B: 0%; $t = 1$ min, A: 100%, B: 0%; $t = 11$ min, A: 92.5%, B: 7.5%. The gradient was slightly tuned to obtain a more efficient separation for β -Man-(1 \rightarrow 3)-Man as follows: $t = 0$ min, A: 100%, B: 0%; $t = 1$ min, A: 100%, B: 0%; $t = 30$ min, A: 92.5%, B: 7.5%. The mobile phase flow rate was set to 300 $\mu\text{L}/\text{min}$ and the volume of the sample injected was 10 μL for all mannobioses. The column eluate was directly infused into the electrospray ionization (ESI) source without any postcolumn addition. The MS conditions were optimized using the built-in semiautomatic tuning procedure in Xcalibur. The ESI source was operated at a temperature of 280 °C with 30 units of sheath gas flow and 10 units of auxiliary gas flow. The ion spray voltage was 4.00 kV, and the transfer capillary temperature was 280 °C. The capillary voltage was 80 V and the tube lens voltage was 150 V. Helium gas was used as the buffer gas for the ion trap as well as the collision gas in CID. The MSⁿ experiments were carried out with a normalized collision energy ranging from 20% to 100%, an activation Q value of 0.25, and a 30-ms activation time. The number of ions regulated by automatic gain control was set to 1×10^5 and the precursor ion isolation width was set to 2 u.

ESI-MSⁿ

All oligosaccharide MSⁿ were obtained using the same mass spectrometer (without HPLC) under similar operating conditions for disaccharides, except the ESI source, which operated at 35 °C, and CID performed at only 30% of normalized collision energy. Samples were prepared at a concentration of 1×10^{-4} M in 50% (v/v%) of HPLC-grade methanol and ultrapure water. Sodium chloride was added to the sample solution at a concentration of 1×10^{-4} M. A total of 1 min of scans was accumulated for each spectral acquisition.

Results and Discussion

Low-energy CID and resonance excitation were used in this study. Sodiated oligosaccharides were dissociated into fragments through sequential low-energy CID and the structures of oligosaccharides were determined using these CID spectra. The spectra were measured according to a procedure that we built from an understanding of the saccharide dissociation mechanism. The linkages, anomeric configurations, and branch locations of oligosaccharides were then determined by comparing the CID spectra of oligosaccharides with the predicted fragmentation patterns and disaccharide database. In the following paragraphs, we first describe the predicted fragmentation patterns, followed by the disaccharide database, the

procedure for CID spectrum measurement, and the applications utilized for the structural determination of oligosaccharides.

Predicted Fragmentation Patterns

In the resonance excitation of low-energy CIDs, only the selected precursor ions were resonance excited to obtain energy from collisions. The internal energy of precursor ions, accumulated through many collisions, increased slowly because the amount of transferred energy in each collision was small. Most ions dissociate through the dissociation channels with low-energy barrier heights before the further increase of internal energy. This ensures that the energy remaining in products after dissociation is insufficient to undergo a secondary dissociation. As product ions are not resonance excited, they do not undergo subsequent excitation and dissociation. The combination of low-energy CID and resonance excitation ensures that only one dissociation process takes place for most ions during each CID.

Fragmentation patterns based on the property of resonance excitation and the dissociation mechanism were used to determine the linkage of the reducing sugar and differentiate the linear and branched oligosaccharides. The fragmentation patterns observed in glucose disaccharides in previous studies [31–34], early semi-empirical calculations [31], and recent high-level quantum chemistry calculations [35] suggest that the retro-Aldol reaction that commences in the O1 atom of the reducing sugar is the dominant mechanism for cross-ring dissociation. Because the retro-Aldol reaction does not depend on the orientation of hydroxyl groups, the same mechanism can be applied to other hexoses, e.g., mannose in this study. The scheme of the retro-Aldol reaction for $^{0,2}A_n$ reaction is shown Scheme 1. For linear oligosaccharides, the presence of $^{0,2}A_n$ fragment ions indicates that the last two monosaccharides at the reducing end is connected by 1→4 or 1→6 linkages, the presence of $^{0,3}A_n$ fragment ions suggests that the last two monosaccharides at the reducing end contain 1→3 or 1→6 linkages, and the presence of $^{0,4}A_n$ fragment ions indicates that the last two monosaccharides at the reducing end demonstrate a 1→6 linkage. When the branch is located on the reducing sugar, the presents of $^{0,2}A_n$ and $^{0,3}A_n$ fragment ions indicate that the linkages at the reducing sugar do not contain (1→3)

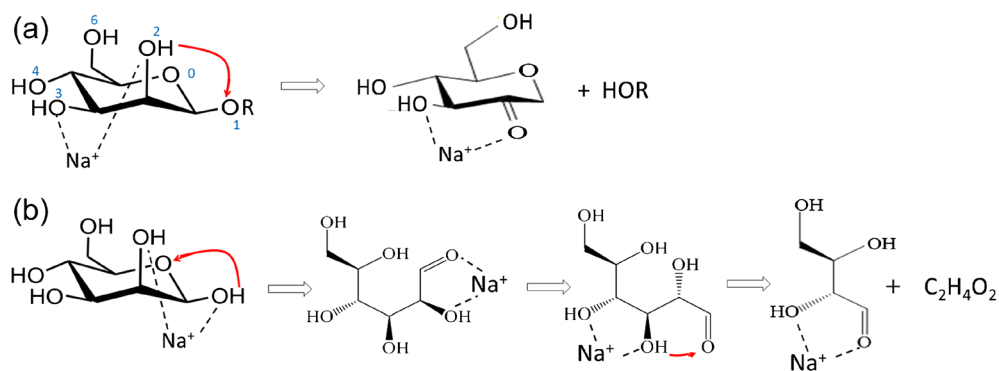
and (1→4) linkages, respectively. Dehydration occurs mainly through the transfer of the H atom from the O2 atom of the reducing sugar to the O1 atom of the same sugar, indicating that this predominantly occurs on the reducing sugar without a (1→2) linkage. The predicted dissociation patterns of trisaccharides based on the mechanisms of cross-ring dissociation and the dehydration reaction are listed in Table 1.

Specially Prepared Disaccharide Database

The process of structural determination includes the dissociation of oligosaccharides into disaccharides through a mass spectrometer and the determination of these disaccharide structures by subsequent CID spectra. In practical applications, the CID spectra of various disaccharides are measured in advance and compiled in a database. The CID spectra of the disaccharides produced from the dissociation of oligosaccharides are compared with those in the disaccharide database to achieve structural identification.

The α and β anomeric configurations at the reducing end of a disaccharide typically coexist in a solution. The ratio of these two configurations depends on the solution conditions (e.g., solvent, pH, and temperature). The CID spectrum of a given disaccharide is the combination spectra of the two anomers, provided they are not separated prior to the CID spectrum measurement. We prepared the database by separating these two anomeric configurations prior to the measurement of the CID spectra. An electrospray linear ion trap mass spectrometer was used to measure the CID spectra directly following the separation of the α and β anomeric configurations through a high-performance liquid chromatography system. The separation of two anomers of each disaccharide is illustrated by the total ion count chromatogram in Figure 1. The corresponding CID spectrum of each peak in the chromatogram is also illustrated in Figure 1.

A major difference between the CID spectra of the disaccharide with 1→3 linkage and the disaccharide with 1→4 linkage is the relative intensity of ion m/z 347, representing the elimination of H_2O from the reducing end. The difference can be explained using the dissociation mechanism. High-level quantum chemistry calculations [8, 35] revealed that the role of sodium cation in the water elimination of sodiated carbohydrates is the promotion of H atom transfer. The mechanism



Scheme 1. (a) Dehydration reaction (R=H) and glycosidic bond cleavage (R=monosaccharide). (b) $^{0,2}A_n$ cross-ring dissociation

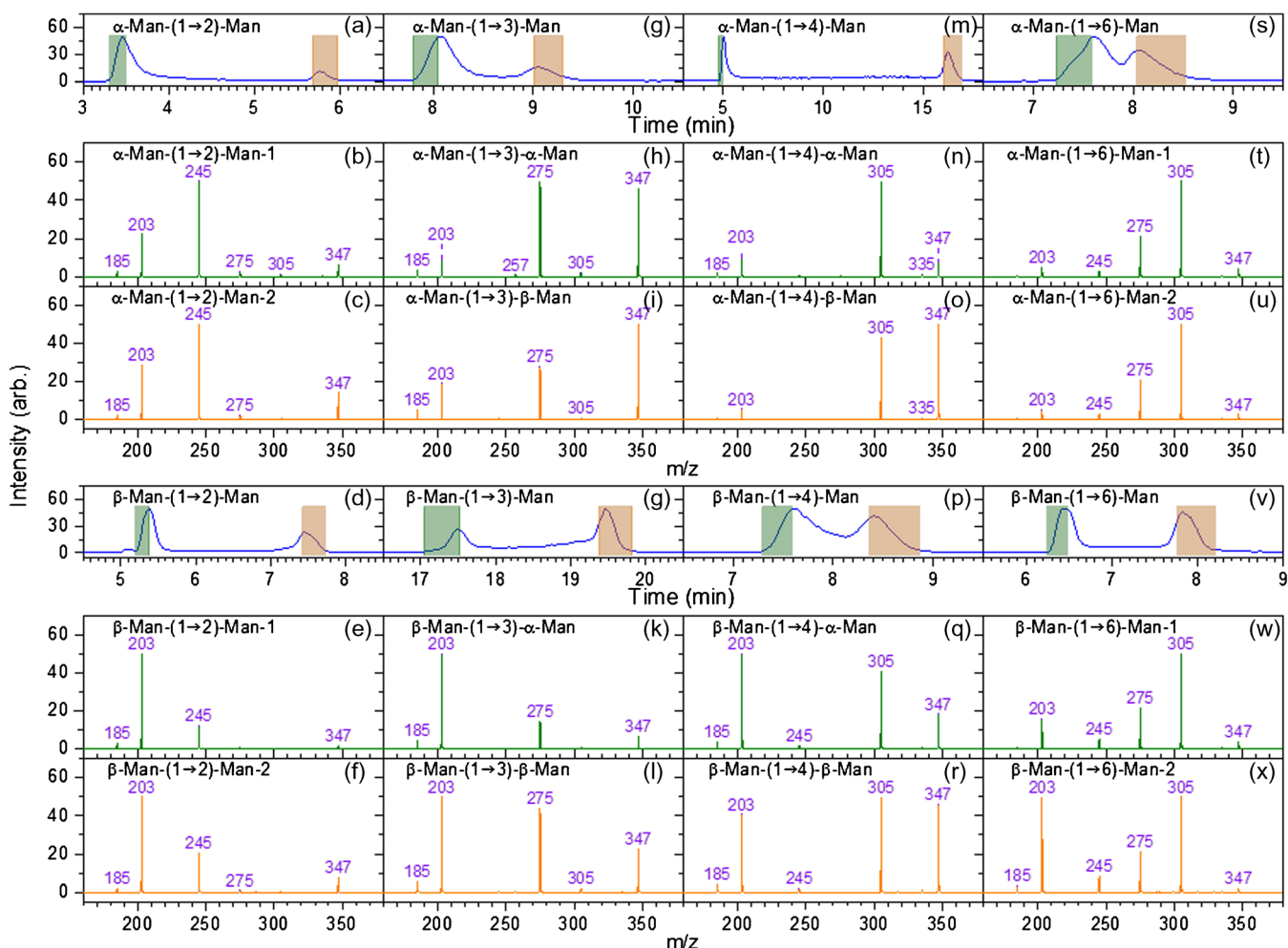


Figure 1. Total ion count chromatograms and CID spectra of various mannose disaccharides. The green and orange areas in each peak of the chromatogram represent the period during which CID spectra were measured. The corresponding spectra are indicated in green and orange, respectively

involves transferring the H atom from the O2 atom of the reducing sugar to the O1 atom of the same sugar, as illustrated in Scheme 1. The barrier height of the O1 and O2 atoms in the cis configuration is substantially lower than that in the trans configuration. Therefore, the CID spectrum with a high intensity of ion m/z 347, which represents the large branching ratio of the dehydration reaction, can be assigned to β anomers. For example, comparing the CID spectra of these two peaks illustrated in Figure 1n and o, the spectrum with a higher intensity of ion m/z 347 (Figure 1o) was assigned to α -Man-(1 \rightarrow 4)- β -Man, whereas the other (Figure 1n) was assigned to α -Man-(1 \rightarrow 4)- α -Man. Similar assignments can be employed for the remaining disaccharides, except for the disaccharides with 1 \rightarrow 2 and 1 \rightarrow 6 linkages, where dehydration is a minor dissociation channel.

A comparison of Figure 1n and q revealed that the major difference in the CID spectra between α -Man-(1 \rightarrow 4)- α -Man and β -Man-(1 \rightarrow 4)- α -Man is the relative intensities of ion m/z 203 and 305. The ion m/z 203 (Y_1) represents glycosidic bond cleavage, and the ion m/z 305 ($^{0,2}A_2$) represents cross-ring dissociation through the elimination of $C_2H_4O_2$ from the

reducing sugar. The difference in spectra can again be explained by the dissociation mechanism due to the cis and trans configurations. The glycosidic bond cleavage mechanism of sodiated carbohydrates is analogous to that of H_2O elimination, as illustrated in Scheme 1. First, the H atom on the O2 atom of the mannose on the nonreducing side of the glycosidic bond is transferred to the O1 atom of the same mannose, and then the C1–O1 glycosidic bond cleavage occurs. The O1 and O2 atoms of the nonreducing mannose in β -Man-(1 \rightarrow 4)- α -Man are in the cis configuration, whereas these two O atoms are in the trans configuration in α -Man-(1 \rightarrow 4)- α -Man. β -Man-(1 \rightarrow 4)- α -Man has a lower barrier height than α -Man-(1 \rightarrow 4)- α -Man; consequently, the intensity of ion m/z 203 of β -Man-(1 \rightarrow 4)- α -Man is higher than that of α -Man-(1 \rightarrow 4)- α -Man. A similar argument can be applied to explain the difference in the CID spectra of other disaccharides.

The measurement of CID spectra for databases was repeated several times to ensure the stability of the relative intensities. The normalized collisional energy (NCE) of CID used in this study ranges from 20% to 100%. The relative ion intensities in each CID spectrum do not change significantly in these

measurements. Spectrum similarities were calculated to identify the stability of the repeated measurements, independence of NCE, and to differentiate the linkages and anomeric configurations. Details of the calculations are displayed in the [Supplementary Information](#).

Procedure of CID Spectrum Measurement

Figure 2 presents the scheme of a procedure to generate the structural decisive fragment ions for the structural determination and subsequent CID spectrum measurements. The first step is the measurement of the MS² spectrum. Ions in regions A, C, and D provide information on the linkage at the reducing sugar and differentiate the linear and branched trisaccharides. The fragmentation patterns of various linear and branched trisaccharides can be found in Table 1. Only the linear trisaccharide with the 1→4 linkage and the branched trisaccharide with the (1→6, 1→4) linkage cannot be distinguished from each other solely according to the ions in regions A, C, and D of the MS² spectrum. However, the subsequent CID spectra, namely MS³(C) and MS³(D) in Figure 2, can be used to distinguish these two trisaccharides.

In the second step, the disaccharide fragment ions in region B represent the disaccharides from both the reducing and nonreducing ends of the linear trisaccharides or the disaccharides from both branches of the branched trisaccharides. The CID spectrum of these ions, namely MS³(B), is the sum of the CID spectra from these two disaccharides. If the structure of one disaccharide is identified, the structure of the other disaccharide can be determined from MS³(B) by subtracting the CID spectrum of the determined disaccharide.

The disaccharide produced in the MS³(C) and MS³(D) is the disaccharide at the nonreducing side of the linear trisaccharides. The CID spectra of this disaccharide, MS⁴(C) and MS⁴(D) (Figure 2) can be used to determine the linkage, the anomeric configuration of the glycosidic bond, and the anomeric configuration of the reducing sugar if the linkage is 1→3 or 1→4 linkage. Notably, the anomeric configuration of the reducing sugar (labeled with 2) of the disaccharide fragment ions produced in MS³(C) and MS³(D) is equivalent to the anomeric configuration of the glycosidic bond between sugars 1 and 2.

The complete structural determination of trisaccharides was obtained by combining the structural information from each step, as illustrated in Figure 2b. One advantage of this method is that most of the structural assignments can be determined through multiple approaches, thus increasing the accuracy of the results.

Applications in Trisaccharides

The procedures involved in structural determination differ slightly depending on the linkages, and can be classified into five types. Herein, we demonstrate how the structures of trisaccharides can be determined for each type.

(1) α -Man-(1→3)- α -Man-(1→6)-Man

The structural determination of α -Man-(1→3)- α -Man-(1→6)-Man is the most common procedure for trisaccharides. The CID spectrum of sodiated α -Man-(1→3)- α -Man-(1→6)-Man is illustrated in Figure 3a. The fragment ions m/z 509, 467, 437, and 407 suggest that the carbohydrate is a linear

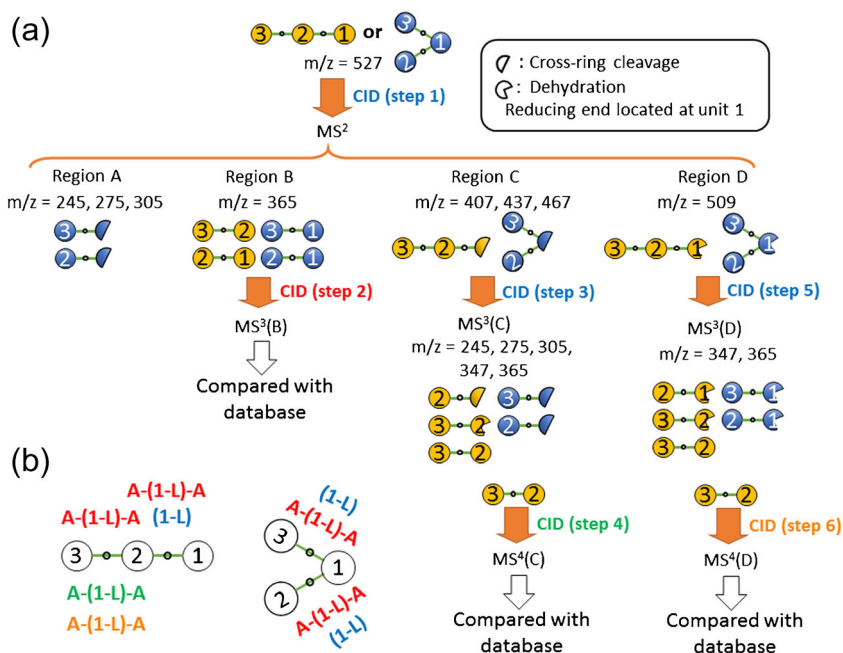


Figure 2. (a) Logical procedures for identifying the structurally decisive ions of trisaccharides and the sequence for low-energy CID measurement. (b) Determinations of the anomeric configuration (A represents α or β) and linkage (L represents 2, 3, 4, or 6) are color coded according to the CID steps of the procedure

Table 1. There are two approaches for the structural determination of α -Man-(1 \rightarrow 2)- α -Man-(1 \rightarrow 3)-Man.

Approach I

Ions m/z 365 produced from $527 \rightarrow 509(B_3) \rightarrow$ fragments (Figure 4b) and $527 \rightarrow 437(^{0,3}A_3) \rightarrow$ fragments (Figure 4c) represent the disaccharide on the nonreducing end of the linear trisaccharide. The CID spectra of these disaccharide fragment ions, $527 \rightarrow 509(B_3) \rightarrow 365(C_2/B_3) \rightarrow$ fragments and $527 \rightarrow 437(^{0,3}A_3) \rightarrow 365(C_2/^0,3A_3) \rightarrow$ fragments, are presented in Figure 4e and f, respectively. A comparison of the spectra in Figure 4e and f with that in Figure 1 suggests that this disaccharide is α -Man-(1 \rightarrow 2)-Man. The anomeric configuration of the reducing sugar of disaccharide α -Man-(1 \rightarrow 2)-Man cannot be determined due to the low dehydration intensity of the disaccharide with 1 \rightarrow 2 linkage. Consequently, the combination of Figure 4a and e or f can only determine the trisaccharide as of α -Man-(1 \rightarrow 2)-Man-(1 \rightarrow 3)-Man. The linkages of both glycosidic bonds and the anomeric configuration of one glycosidic bond were identified, but the determination of the other anomeric configuration required a different approach.

Approach II

The disaccharides produced from $527 \rightarrow 365(C_2 \text{ or } Y_2)$ (Figure 4d) include the disaccharides on both the reducing and nonreducing sides. As the disaccharide on the nonreducing side was determined to be α -Man-(1 \rightarrow 2)-Man in the aforementioned approach (Figure 4e and f), subtracting Figure 4e or f from d generated the CID spectrum of the disaccharide on the reducing side (Figure 4g or h), which can be identified as α -Man-(1 \rightarrow 3)-Man from the comparison with Figure 1. Therefore the structure of this trisaccharide can be completely determined to be α -Man-(1 \rightarrow 2)- α -Man-(1 \rightarrow 3)-Man by approach II through combining Figure 4a, d, and either g or h.

(3) β -Man-(1 \rightarrow 4)- β -Man-(1 \rightarrow 4)-Man

The MS² spectrum of sodiated β -Man-(1 \rightarrow 4)- β -Man-(1 \rightarrow 4)-Man is illustrated in Figure 5a. The ions m/z 509 and 467 suggested that the carbohydrate is a linear trisaccharide

with a 1 \rightarrow 4 linkage or a branched trisaccharide with 1 \rightarrow 4 and 1 \rightarrow 6 linkages on the reducing sugar, according to the fragmentation patterns shown in Table 1.

Ion m/z 365 in the CID spectrum of $527 \rightarrow 509(B_3) \rightarrow$ fragments (Figure 5b) or ion m/z 347 in the CID spectrum of $527 \rightarrow 467(^{0,2}A_3) \rightarrow$ fragments (Figure 5c) indicates that the trisaccharide is a linear oligosaccharide, according to the logical procedures illustrated in Figure 2 and the fragmentation patterns in Table 1. The CID spectrum of $527 \rightarrow 509(B_3) \rightarrow 365(C_2/B_3) \rightarrow$ fragments is presented in Figure 5d. A comparison of the spectrum in Figure 5d with that in Figure 1 suggested that this disaccharide is β -Man-(1 \rightarrow 4)- β -Man. The combination of mass spectra in Figure 5a, b, c, and d determines the linkage position and anomeric configuration of this trisaccharide as β -Man-(1 \rightarrow 4)- β -Man-(1 \rightarrow 4)-Man.

(4) α -Man-(1 \rightarrow 6)- α -Man-(1 \rightarrow 6)-Man

The CID spectrum of sodiated α -Man-(1 \rightarrow 6)- α -Man-(1 \rightarrow 6)-Man is illustrated in Figure 6a. The ions m/z 509, 467, 437, and 407 indicate that the carbohydrate is a linear trisaccharide with a 1 \rightarrow 6 linkage on the reducing sugar, according to the fragmentation patterns in Table 1. Ions m/z 365 produced from $527 \rightarrow 509(B_3) \rightarrow$ fragments (Figure 6b), $527 \rightarrow 467(^{0,2}A_3) \rightarrow$ fragments (Figure 6c), and $527 \rightarrow 437(^{0,3}A_3) \rightarrow$ fragments (Figure 6d) all represent the disaccharide on the nonreducing end of the linear trisaccharide. The CID spectra of this disaccharide fragment ion, namely $527 \rightarrow 509(B_3) \rightarrow 365(C_2/B_3) \rightarrow$ fragments, $527 \rightarrow 467(^{0,2}A_3) \rightarrow 365(C_2/^0,2A_3) \rightarrow$ fragments, and $527 \rightarrow 437(^{0,3}A_3) \rightarrow 365(C_2/^0,3A_3) \rightarrow$ fragments are presented in Figure 6e, f, and g, respectively. A comparison of the spectra in Figure 6e, f, and g with that in Figure 1 suggests that this disaccharide is α -Man-(1 \rightarrow 6)-Man. The combination of mass spectra in Figure 6a and any one of the spectra in Figure 6e, f, or g determines the linkage position and anomeric configuration of this trisaccharide as α -Man-(1 \rightarrow 6)-Man-(1 \rightarrow 6)-Man. Similar to the structural determination of α -Man-(1 \rightarrow 2)- α -Man-(1 \rightarrow 3)-Man, the anomeric configuration of the glycosidic bond on the reducing end of α -Man-(1 \rightarrow 6)-Man-(1 \rightarrow 6)-Man

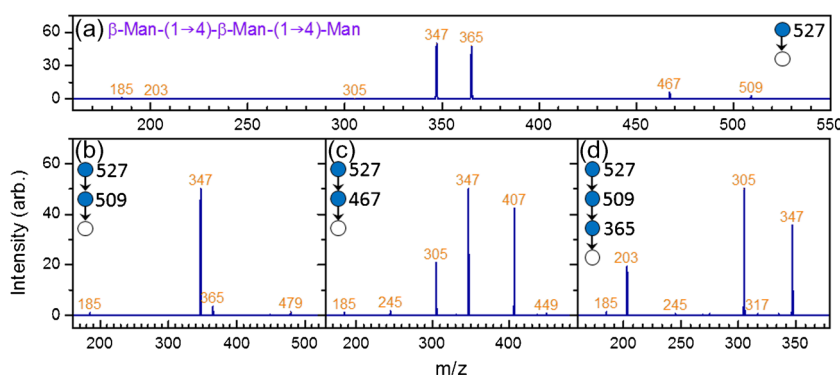


Figure 5. CID spectra of β -Man-(1 \rightarrow 4)- β -Man-(1 \rightarrow 4)-Man

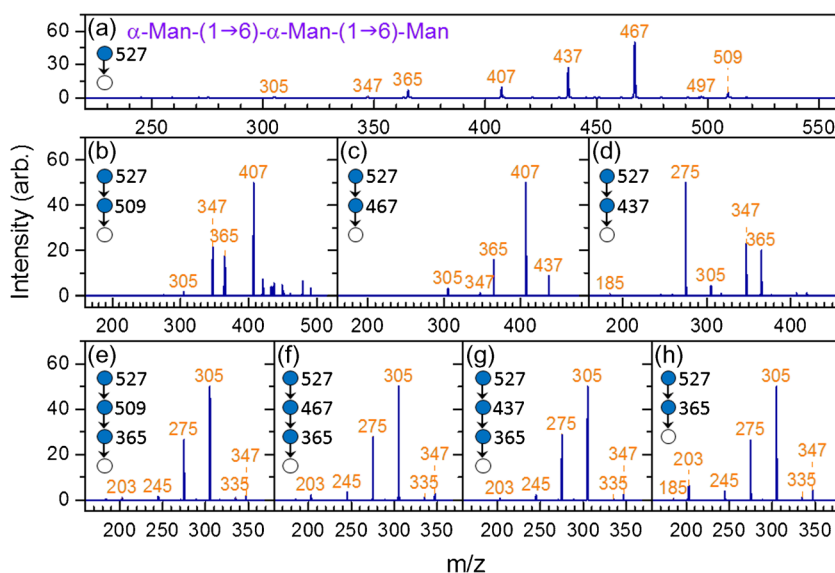


Figure 6. CID spectra of α -Man-(1 \rightarrow 6)- α -Man-(1 \rightarrow 6)-Man

cannot be determined due to the low dehydration intensity of disaccharide with 1 \rightarrow 6 linkage.

The analogous method of approach II for α -Man-(1 \rightarrow 2)- α -Man-(1 \rightarrow 3)-Man does not achieve desirable results for α -Man-(1 \rightarrow 6)- α -Man-(1 \rightarrow 6)-Man because the linkages of both glycosidic bonds are the same (1 \rightarrow 6). The identification of the anomeric configuration of the glycosidic bond on the reducing end requires another approach.

The alternative approach employs the ^{18}O labeled α -Man-(1 \rightarrow 6)- α -Man-(1 \rightarrow 6)-Man. Figure 7a shows the CID spectra of α -Man-(1 \rightarrow 6)- α -Man-(1 \rightarrow 6)-Man, in which ^{18}O is labeled at the O1 position of the reducing sugar. The CID spectra of the 529 \rightarrow 365(C_2) \rightarrow fragments (Figure 7e) and 529 \rightarrow 367(Y_2) \rightarrow fragments (Figure 7i) suggest that the disaccharides on both the reducing and nonreducing sides are α -Man-(1 \rightarrow 6)-Man. The

combination of these two disaccharides indicates that the trisaccharide is α -Man-(1 \rightarrow 6)- α -Man-(1 \rightarrow 6)-Man.

(5) α -Man-(1 \rightarrow 3)-[α -Man-(1 \rightarrow 6)]-Man

Most current de novo structural determination methods are only applicable in linear oligosaccharides. The structural identification of branched oligosaccharides remains a significant challenge. The CID spectrum of sodiated α -Man-(1 \rightarrow 3)-[α -Man-(1 \rightarrow 6)]-Man, a branched trisaccharide, is illustrated in Figure 8a. The ions m/z 509 and 275 indicate that the carbohydrate is a branched trisaccharide with 1 \rightarrow 3 and 1 \rightarrow 6 linkages on the reducing sugar, according to the fragmentation patterns in Table 1. The comparison of fragmentation patterns in Table 1 with the ions m/z 347 produced from

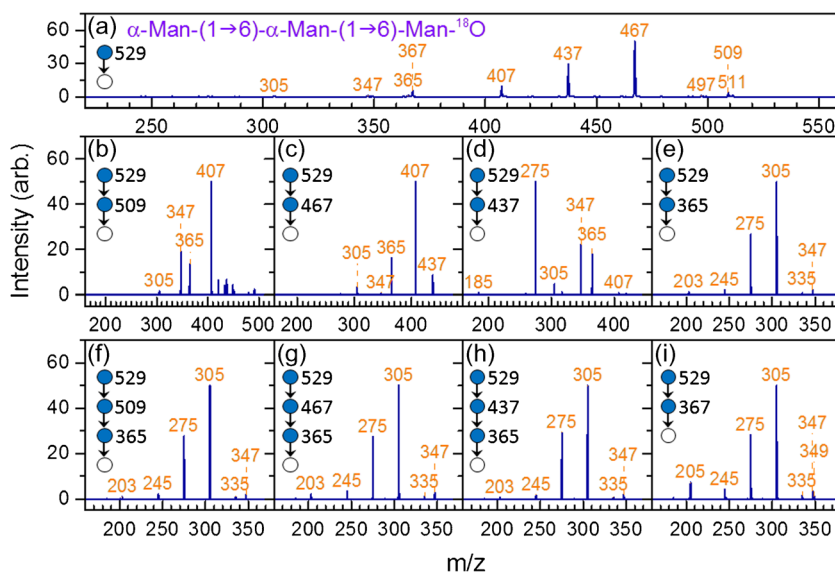


Figure 7. CID spectra of ^{18}O labeled α -Man-(1 \rightarrow 6)- α -Man-(1 \rightarrow 6)-Man. ^{18}O is labeled at the O1 position of the reducing sugar

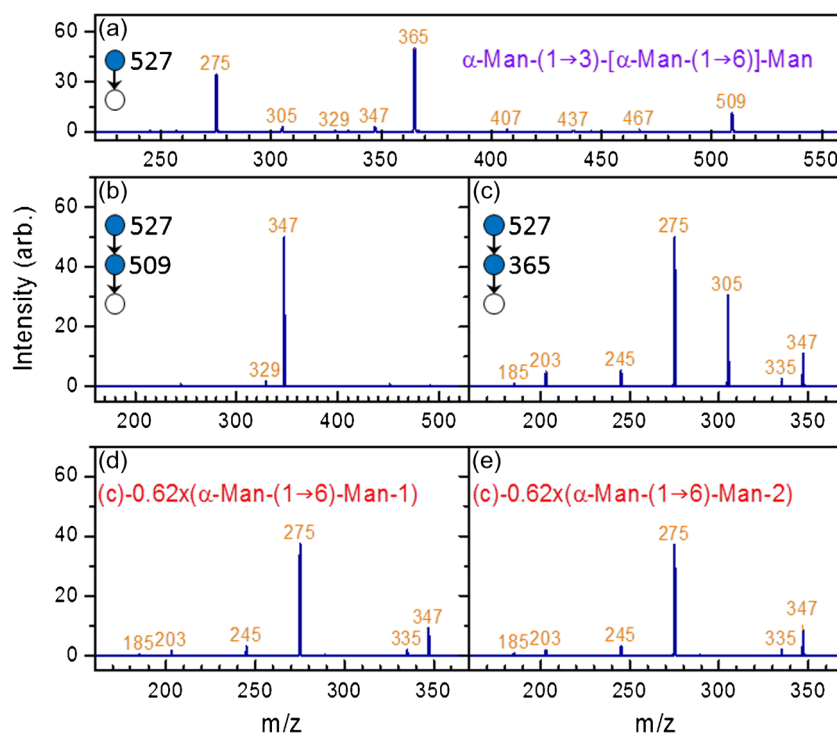


Figure 8. CID spectra of α -Man-(1 \rightarrow 3)-[α -Man-(1 \rightarrow 6)]-Man. Spectrum in (d) and (e) were produced by subtracting the weighted spectrum in Figure 1t and u from that in (c), respectively. The weighted factor was chosen such that ion m/z 305 has zero intensity in (d) and (e)

527 \rightarrow 509 \rightarrow fragments (Figure 8b) provide additional confirmation of the linkages on the reducing sugar.

The CID spectrum of 527 \rightarrow 365 \rightarrow fragments (Figure 8c) is the sum of the spectra of disaccharides with 1 \rightarrow 3 and 1 \rightarrow 6 linkages. Subtraction of the spectrum with 1 \rightarrow 6 linkage (Figure 1t, u, w, or x) from that in Figure 8c yields a spectrum with 1 \rightarrow 3 linkage. In the subtraction process, ion intensities in Figure 1t, u, w, or x must be multiplied by a factor such that the spectrum after subtraction exhibits a near-zero intensity for ions m/z 245 and 305. This is because the spectrum after subtraction yields a spectrum of disaccharide with 1 \rightarrow 3 linkage, which requires a near-zero intensity for ions m/z 245 and 305, as illustrated in the disaccharide database of Figure 1. If Figure 1w or x (β -Man-(1 \rightarrow 6)-Man-1 or β -Man-(1 \rightarrow 6)-Man-2) is used in subtraction, the ion intensity m/z 203 in the spectrum after subtraction displays negative values. Consequently, only Figure 1t and u (α -Man-(1 \rightarrow 6)-Man-1 or α -Man-(1 \rightarrow 6)-Man-2) can be used for subtraction. The subtraction of Figure 1t or u from Figure 8b is shown in Figure 8d and e, respectively, which indicates that the disaccharide is α -Man-(1 \rightarrow 3)- α -Man through the comparison of the spectrum in Figure 8d and e with that in Figure 1. The combination of these CID spectra determined the trisaccharide as α -Man-(1 \rightarrow 3)-[α -Man-(1 \rightarrow 6)]-Man.

Conclusions

Currently, the identification of the linkage positions, anomeric configurations, and branching location of oligosaccharides is a

major obstacle to carbohydrate research. In this study, we demonstrated a simple approach for the structural determination of underivatized mannose trisaccharides. The structural determination followed a logical procedure built from the understanding of the saccharide dissociation mechanism. This logical procedure can be easily extended to larger oligosaccharides and those containing hexoses other than mannose. The ion intensities of sodiated carbohydrates are high and the entire measurement of tandem MS can take less than 1 min. This method can be ultimately developed into a standard procedure for the structural identification of oligosaccharides and complex carbohydrates, a goal that remains a great challenge in glycomic analysis.

Acknowledgments

This work was financially supported in part by the Ministry of Science and Technology, Taiwan (103-2113-M-001-011-NY3).

References

1. Varki, A., Cummings, R.D., Esko, J.D., Freeze, H.H., Stanley, P., Bertozzi, C.R., Hart, G.W., Etzler, M.E. (eds.): *Essentials of Glycobiology*, 2nd edn. Cold Spring Harbor Laboratory Press, Cold Spring Harbor (2009)
2. Bertozzi, C.R., Kiessling, L.L.: Chemical glycobiology. *Science* **291**(5512), 2357–2364 (2001)
3. National Research Council: *Transforming Glycoscience: A Roadmap for the Future*. The National Academies Press, Washington, DC (2012)

4. Laine, R.A.: A Calculation of All Possible Oligosaccharide Isomers Both Branched and Linear Yields 1.05×10^{12} Structures for a Reducing Hexasaccharide - the Isomer-Barrier to Development of Single-Method Saccharide Sequencing or Synthesis Systems. *Glycobiology*. **4**(6), 759–767 (1994)
5. Duus, J.O., Gotfredsen, C.H., Bock, K.: *Chem. Rev.* **100**, 4589 (2000)
6. Kailemia, M.J., Ruhaak, L.R., Lebrilla, C.B., Amster, I.J.: Oligosaccharide analysis by mass spectrometry: a review of recent developments. *Anal. Chem.* **86**(1), 196–212 (2014)
7. Naven, T.J., Harvey, D.J.: Effect of structure on the signal strength of oligosaccharides in matrix-assisted laser desorption/ionization mass spectrometry on time-of-flight and magnetic sector instruments. *Rapid Commun. Mass Spectrom.* **10**(11), 1361–1366 (1996)
8. Chen, J.L., Lee, C., Lu, I.C., Chien, C.L., Lee, Y.T., Hu, W.P., Ni, C.K.: Theoretical investigation of low detection sensitivity for underivatized carbohydrates in ESI and MALDI. *J. Mass Spectrom.* **51**(12), 1180–1186 (2016)
9. Zaia, J.: Mass spectrometry of oligosaccharides. *Mass Spectrom. Rev.* **23**(3), 161–227 (2004)
10. Stephens, E., Maslen, S.L., Green, L.G., Williams, D.H.: Fragmentation characteristics of neutral N-linked glycans using a MALDI-TOF/TOF tandem mass spectrometer. *Anal. Chem.* **76**(8), 2343–2354 (2004)
11. Kurimoto, A., Daikoku, S., Mutsuga, S., Kanie, O.: Analysis of energy-resolved mass spectra at MS n in a pursuit to characterize structural isomers of oligosaccharides. *Anal. Chem.* **78**(10), 3461–3466 (2006)
12. Vijaykrishnan, B., Issaree, A., Corilo, Y.E., Ferreira, C.R., Eberlin, M.N., Peter, M.G.: MSⁿ of the six isomers of (GlcN)₂(GlcNAc)₂ aminoglucon tetrasaccharides (diacetylchitotetraoses): Rules of fragmentation for the sodiated molecules and application to sequence analysis of hetero-chitooligosaccharides. *Carbohydr. Polym.* **84**(2), 713–726 (2011)
13. Li, D.T., Her, G.R.: Structural analysis of chromophore-labeled disaccharides and oligosaccharides by electrospray ionization mass spectrometry and high-performance liquid chromatography/electrospray ionization mass spectrometry. *J. Mass Spectrom.* **33**(7), 644–652 (1998)
14. Cheng, H.L., Her, G.R.: Determination of linkages of linear and branched oligosaccharides using closed-ring chromophore labeling and negative ion trap mass spectrometry. *J. Am. Soc. Mass. Spectrom.* **13**(11), 1322–1330 (2002)
15. Harvey, D.J.: Fragmentation of negative ions from carbohydrates: Part 1. Use of nitrate and other anionic adducts for the production of negative ion electrospray spectra from N-linked carbohydrates. *J. Am. Soc. Mass. Spectrom.* **16**(5), 622–630 (2005)
16. Harvey, D.J.: Fragmentation of negative ions from carbohydrates: part 2. Fragmentation of high-mannose N-linked glycans. *J. Am. Soc. Mass Spectrom.* **16**(5), 631–646 (2005)
17. Guan, B., Cole, R.B.: MALDI linear-field reflectron TOF post-source decay analysis of underivatized oligosaccharides: Determination of glycosidic linkages and anomeric configurations using anion attachment. *J. Am. Soc. Mass. Spectrom.* **19**(8), 1119–1131 (2008)
18. Harvey, D.J., Jaeken, J., Butler, M., Armitage, A.J., Rudd, P.M., Dwek, R.A.: Fragmentation of negative ions from N-linked carbohydrates, part 4. Fragmentation of complex glycans lacking substitution on the 6-antenna. *J. Mass Spectrom.* **45**(5), 528–535 (2010)
19. Viseux, N., de Hoffmann, E., Domon, B.: Structural assignment of permethylated oligosaccharide subunits using sequential tandem mass spectrometry. *Anal. Chem.* **70**(23), 4951–4959 (1998)
20. van der Kerk, S.M., Blok-Tip, L., van der Kerk-van Hoof, A., Heerma, W., Haverkamp, J.: Differences in fragmentation behaviour between α - and β -linked derivatized xylobiosides: explanation in terms of sigma conjugation. *Int. J. Mass Spectrom. Ion Processes.* **134**(1), 41–54 (1994)
21. Xue, J., Song, L., Khaja, S.D., Locke, R.D., West, C.M., Laine, R.A., Matta, K. L.: Determination of linkage position and anomeric configuration in Hex-Fuc disaccharides using electrospray ionization tandem mass spectrometry. *Rapid Commun. Mass Spectrom.* **18**(17), 1947–1955 (2004)
22. Mendonca, S., Cole, R.B., Zhu, J., Cai, Y., French, A.D., Johnson, G.P., Laine R.A.: Incremented alkyl derivatives enhance collision induced glycosidic bond cleavage in mass spectrometry of disaccharides. *J. Am. Soc. Mass. Spectrom.* **14**(1), 63–78 (2003)
23. Ashline, D., Singh, S., Hanneman, A., Reinhold, V.: Congruent strategies for carbohydrate sequencing. 1. Mining structural details by MS n. *Anal. Chem.* **77**(19), 6250–6262 (2005)
24. Zhang, H., Singh, S., Reinhold, V.N.: Congruent strategies for carbohydrate sequencing. 2. FragLib: An MS n spectral library. *Anal. Chem.* **77**(19), 6263–6270 (2005)
25. Nagy, G., Pohl, N.L.: Complete hexose isomer identification with mass spectrometry. *J. Am. Soc. Mass. Spectrom.* **26**(4), 677–685 (2015)
26. Fang, T.T., Zirrolli, J., Bendiak, B.: Differentiation of the anomeric configuration and ring form of glucosyl-glycolaldehyde anions in the gas phase by mass spectrometry: isomeric discrimination between m/z 221 anions derived from disaccharides and chemical synthesis of m/z 221 standards. *Carbohydr. Res.* **342**(2), 217–235 (2007)
27. Fang, T.T., Bendiak, B.: The stereochemical dependence of unimolecular dissociation of monosaccharide-glycolaldehyde anions in the gas phase: a basis for assignment of the stereochemistry and anomeric configuration of monosaccharides in oligosaccharides by mass spectrometry via a key discriminatory product ion of disaccharide fragmentation, m/z 221. *J. Am. Chem. Soc.* **129**(31), 9721–9736 (2007)
28. Konda, C., Londry, F.A., Bendiak, B., Xia, Y.: Assignment of the Stereochemistry and Anomeric Configuration of Sugars within Oligosaccharides Via Overlapping Disaccharide Ladders Using MSn. *J. Am. Soc. Mass. Spectrom.* **25**(8), 1441–1450 (2014)
29. Ni, C.K.: Simple methods for de novo structural determination of glucose-containing underivatized oligosaccharides. In the division of carbohydrate chemistry, 254th American Chemical Society National Meeting & Exposition August 20–24, 2017, Washington, DC USA
30. Konda, C., Bendiak, B., Xia, Y.: Differentiation of the stereochemistry and anomeric configuration for 1-3 linked disaccharides via tandem mass spectrometry and ¹⁸O-labeling. *J. Am. Soc. Mass. Spectrom.* **23**(2), 347–358 (2012)
31. Hofmeister, G.E., Zhou, Z., Leary, J.A.: Linkage Position Determination in Lithium-Cationized Disaccharides - Tandem Mass-Spectrometry and Semiempirical Calculations. *J. Am. Chem. Soc.* **113**(16), 5964–5970 (1991)
32. Asam, M.R., Glish, G.L.: Tandem mass spectrometry of alkali cationized polysaccharides in a quadrupole ion trap. *J. Am. Soc. Mass. Spectrom.* **8**(9), 987–995 (1997)
33. da Costa, E.V., Moreira, A.S., Nunes, F.M., Coimbra, M.A., Evtuguin, D.V., Domingues, M.R.: Differentiation of isomeric pentose disaccharides by electrospray ionization tandem mass spectrometry and discriminant analysis. *Rapid Commun. Mass Spectrom.* **26**(24), 2897–2904 (2012)
34. Zhang, H., Brokman, S.M., Fang, N., Pohl, N.L., Yeung, E.S.: Linkage position and residue identification of disaccharides by tandem mass spectrometry and linear discriminant analysis. *Rapid Commun. Mass Spectrom.* **22**(10), 1579–1586 (2008)
35. Chen, J.L., Nguan, H.S., Hsu, P.J., Tsai, S.T., Liew, C.Y., Kuo, J.L., Hu, W.P., Ni, C.K.: Collision-induced dissociation of sodiated glucose and identification of anomeric configuration. *Phys. Chem. Chem. Phys.* **19**, 15454–15462 (2017)